11th International Fermi Symposium
College Park, Maryland, USA, September 9-13, 2024

On non-detection of Gamma-Ray Bursts in three compact binary merger events detected by LIGO

Soebur Razzaque

UNIVERSITY OF JOHANNESBURG

CAPP
Centre for Astro-Particle Physics

THE GEORGE WASHINGTON UNIVERSITY
WASHINGTON, DC

Fermi Gamma-ray Space Telescope

SA-GAMMA
THE SOUTH AFRICAN GAMMA-RAY ASTRONOMY PROGRAMME

NRF National Research Foundation

GW170817 and GRB 170817A

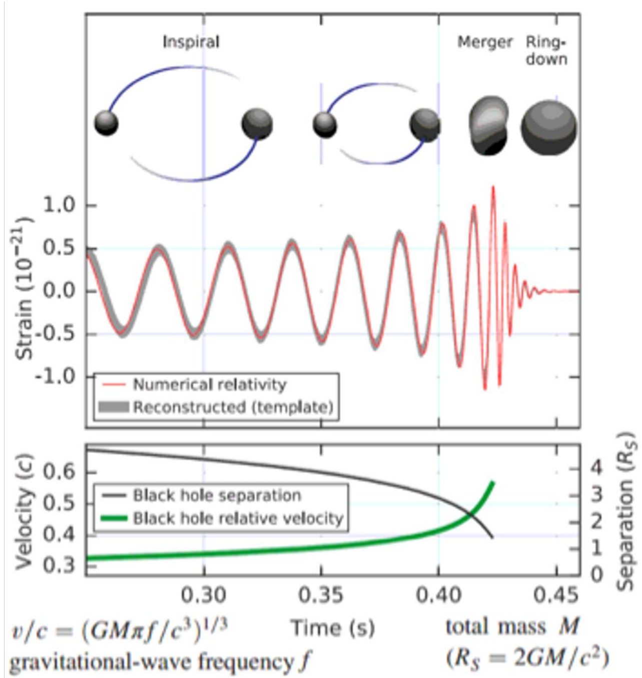

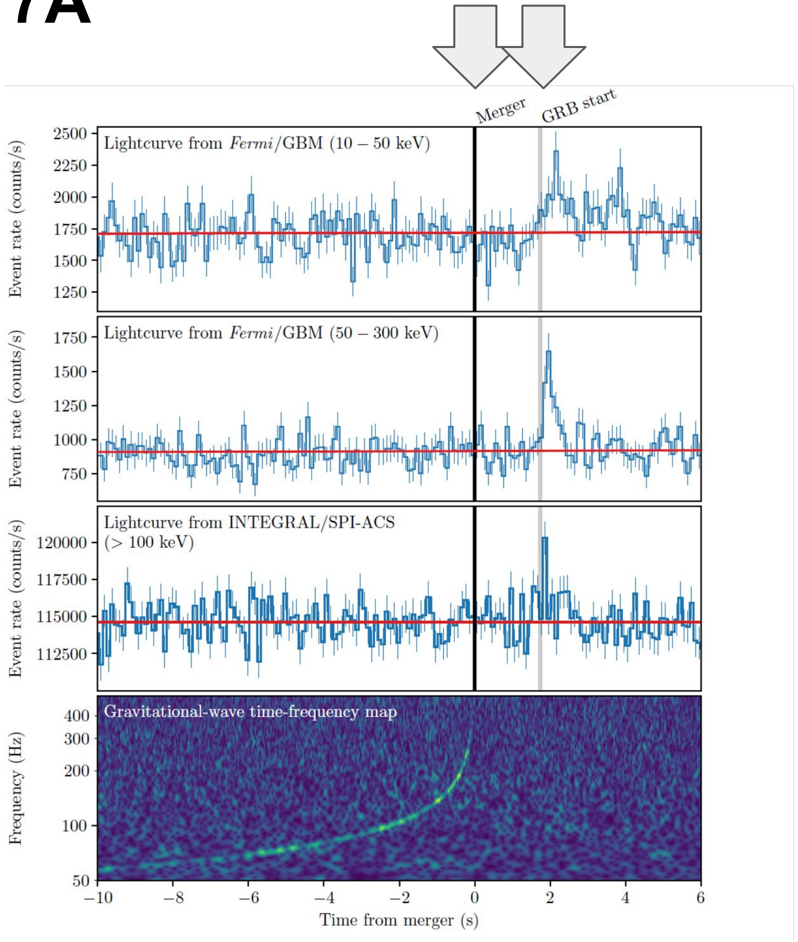

LIGO & Virgo Collaborations 2017

GW170817 and GRB 170817A

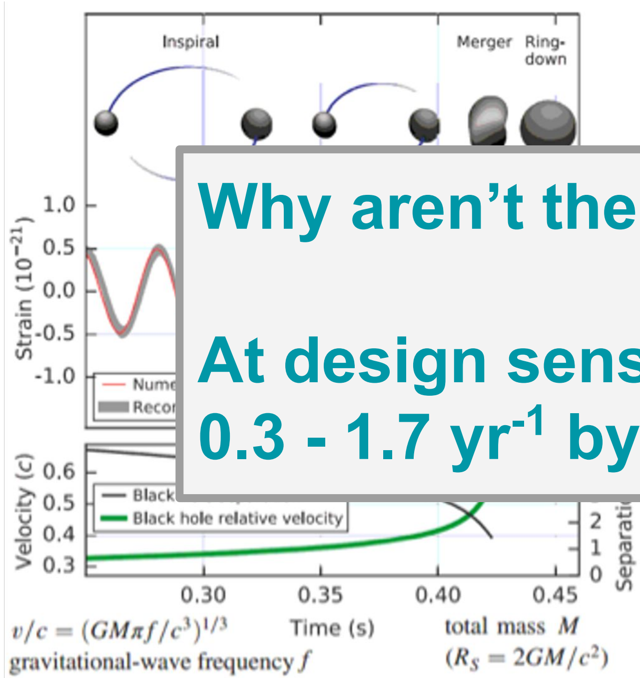

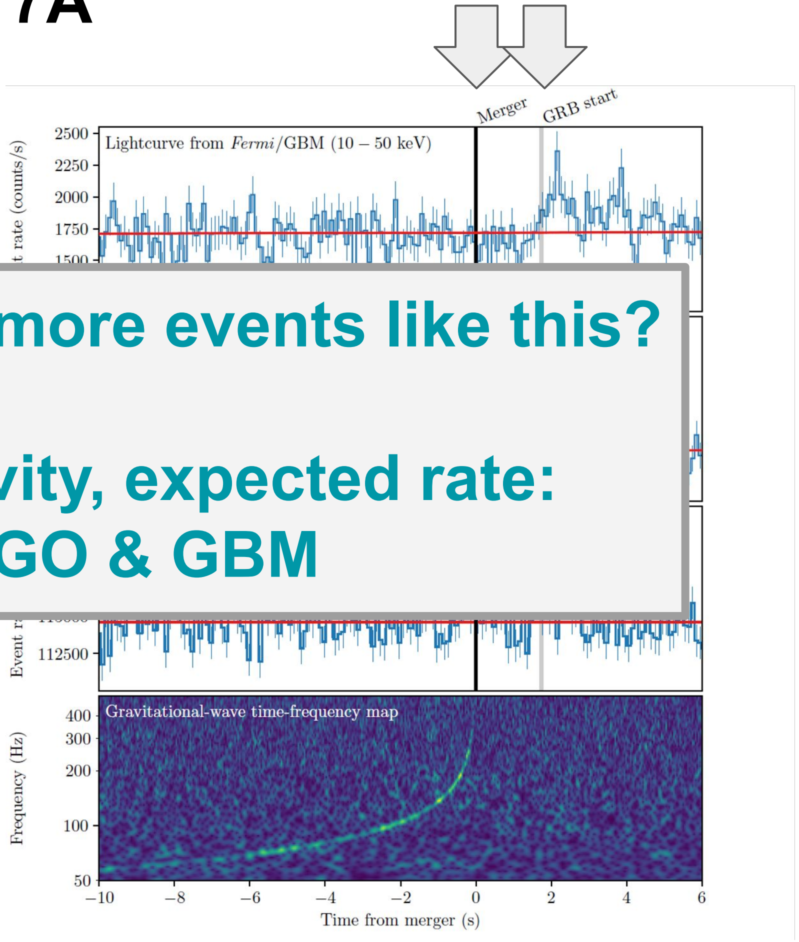

Why aren't there more events like this?

At design sensitivity, expected rate:
0.3 - 1.7 yr^{-1} by LIGO & GBM

LIGO & Virgo Collaborations 2017

GW-GRB joint detection

During LIGOs O2 and O3:

- A second Binary Neutron Star (BNS) merger **GW190425** and
- Five Black Hole Neutron Star (BHNS) mergers **GW190917_114636,** *GW191219_163120,* **GW200115_042309,** *GW200210_114636* and *GW200105 162426*

A few of these events could be possible sources for a GRB but no electromagnetic counterpart were detected.

GW-GRB joint detection

During LIGOs O2 and O3:

- A second Binary Neutron Star (BNS) merger **GW190425** and
- Five Black Hole Neutron Star (BHNS) mergers **GW190917_114636,** *GW191219_163120,* **GW200115_042309,** *GW200210_114636* and *GW200105 162426*

A few of these events could be possible sources for a GRB but no electromagnetic counterpart were detected.

Possible explanations for the lack of further GW/GRB joint detections

1. Sub luminous GRB events like GRB170817A can only be detected up to about 80 Mpc [*Abbott+2017*].
2. Secondly, depending on the location of the source, it's possible that the source was outside the field of view of Fermi-GBM/Swift [*Fletcher+2024*].

A third possibility

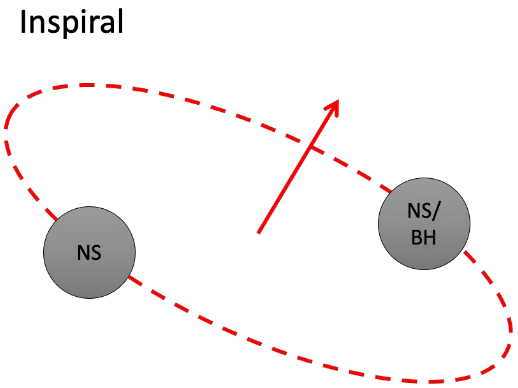

From GW170817
and GRB 170817A
Observations

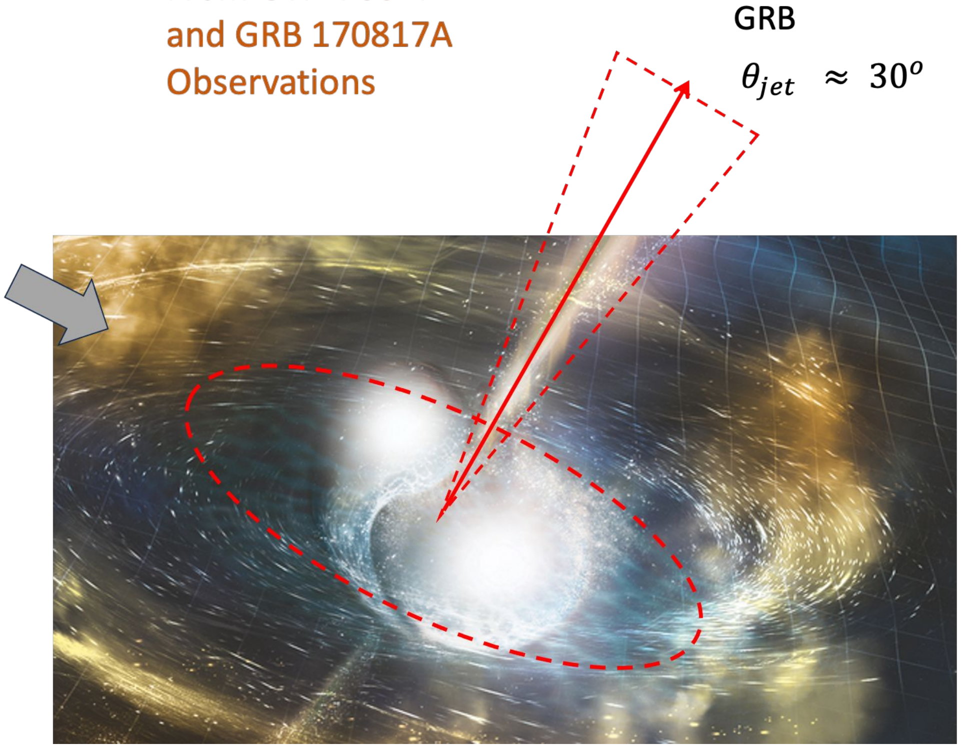

Credit: LIGO/VIRGO Collab.

- Only a fraction of GW events would be detected as GRBs
- Joint detection or non-detection is extremely useful

Methodology

- We performed Bayesian inference on the following GW events
  BNS events: **GW170817, GW190425**
  BHNS events: **GW190917_114636, GW2000115_042309**
- Used **Bilby** which is python based Bayesian inference library for GW astronomy [*Ashton+2019*]
- GW170817 has an observed EM counterpart GRB170817A. As a result, the inclination angle is well constrained. To test how effective pure GW analysis is using Bilby, we aimed to obtain similar values for the inclination angle through pure GW analysis.
- To perform Bayesian analysis, we define a prior giving the distribution of the waveform parameters. Following convention, we set up two priors that represent a low spin and high spin case for the merger.

Luyanda Mazwi (MSc work)

*Luyanda Mazwi, SR & Lutendo Nyadzani, MNRAS **531,** 2162 (2024)*

Waveforms

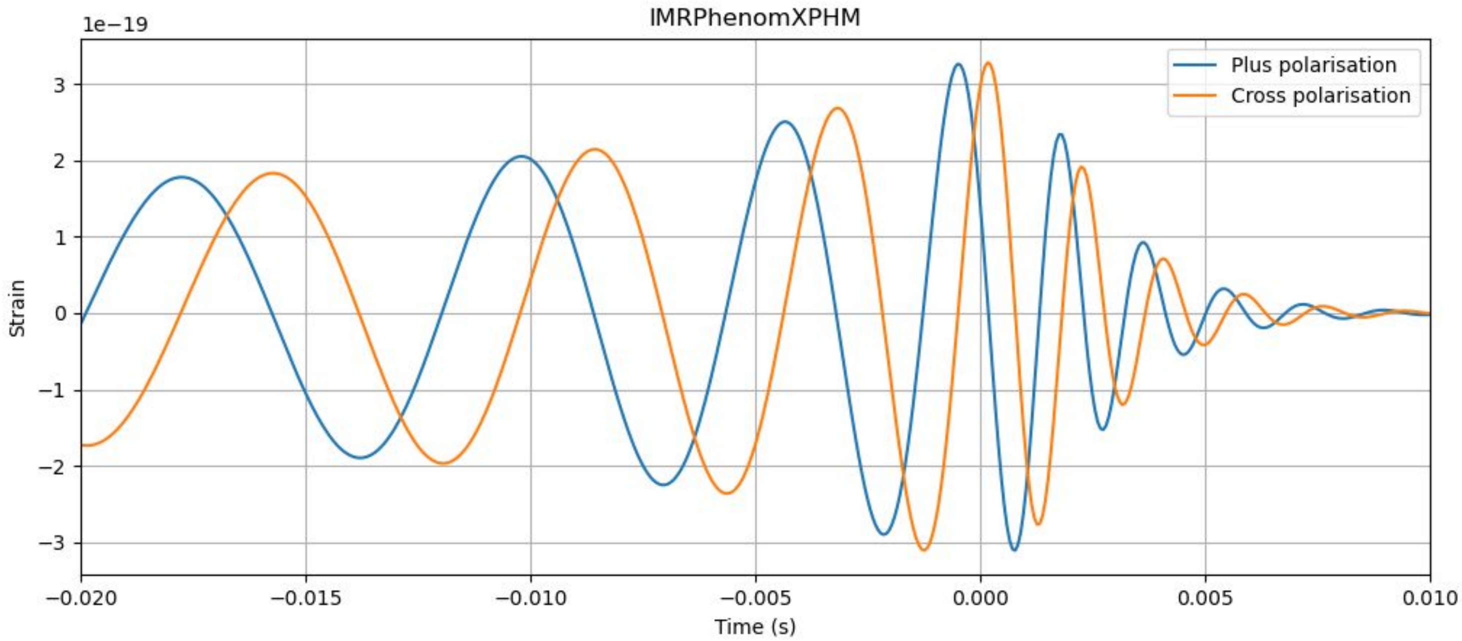
IMRPhenomXPHM
1e−19
Plus polarisation
Cross polarisation
Strain
3
2
1
0
−1
−2
−3
−0.020
−0.015
−0.010
−0.005
0.000
0.005
0.010
Time (s)

Waveform models

- **Frequency domain waveform models were used to perform the analysis.**
  - **BNS mergers: IMRPhenomPv2_NRTidal, IMRPhenomD_NRTidal and TaylorF2.**
  - **BHNS mergers: IMRPhenomPv2 and IMRPhenomXPHM.**

- TaylorF2 is an analytical Post-Newtonian (PN) model for GWs from non-spinning binaries in the quasi-circular inspiral phase in the frequency domain. Corrections up to 3.5 PN and is computed in the stationary phase approximation (SPA) [Heurta+2014].
- Remaining 3 waveforms are all Inspiral Merger Ringdown (IMR) based on phenomenological (Phenom) treatments of the IMR.
- IMRPhemomD is a model based on aligned spin point particle models tuned to Numerical Relativity (NR) hybrids and Effective One Body (EOB) wave forms [Abott+2019]
- IMRPhenomP includes spin precession [Abott+2019]
- IMRPhenomXPHM models GWs from a quasi circular precessing BBH [Pratten+2021].

Choice of priors on inclination and distance

Parameter		**Low spin prior ($\chi \leq 0.05$)**	**High spin prior ($\chi \leq 0.89$)**
Inclination ι	GW190425	uniform prior: 0° ≤ ι ≤ 90°	Uniform prior: 0° ≤ ι ≤ 90°
	GW190917	Uniform prior: 0° ≤ ι ≤ 90° & Sinusoidal prior: 0° ≤ ι ≤ 360°	Uniform prior: 0° ≤ ι ≤ 90° & Sinusoidal prior: 0° ≤ ι ≤ 360°
	GW200115	Uniform prior: 0° ≤ ι ≤ 90° & Sinusoidal prior: 0° ≤ ι ≤ 360°	Uniform prior: 0° ≤ ι ≤ 90° & Sinusoidal prior: 0° ≤ ι ≤ 360°
Luminosity distance D	GW190425	Uniform prior: 104 Mpc ≤ D ≤ 188 Mpc	Uniform prior: 104 Mpc ≤ D ≤ 188 Mpc
	GW190917	Power law with Index α= 2: 410 Mpc ≤ D ≤ 1060 Mpc	Power law with Index α= 2: 410 Mpc ≤ D ≤ 1060 Mpc
	GW200115	Power law with Index α= 2: 202 Mpc ≤ D ≤ 352 Mpc	Power law with Index α= 2: 202 Mpc ≤ D ≤ 352 Mpc

Results of Bayesian analysis

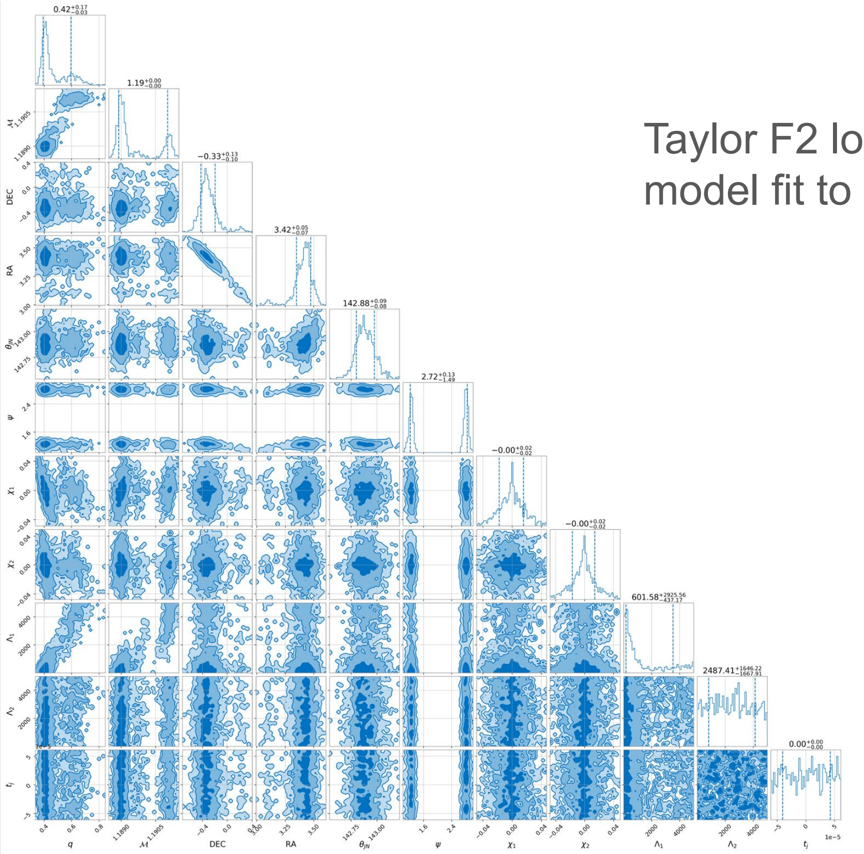

Taylor F2 low-spin waveform model fit to GW170817 data

Results on the inclination: GW170817 (BNS)

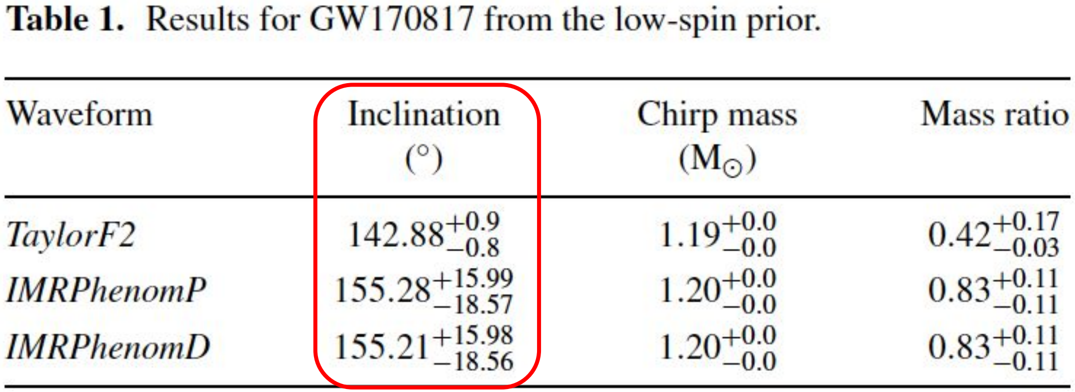

Table 1. Results for GW170817 from the low-spin prior.

Waveform	Inclination (°)	Chirp mass ($M_\odot$)	Mass ratio
TaylorF2	$142.88^{+0.9}_{-0.8}$	$1.19^{+0.0}_{-0.0}$	$0.42^{+0.17}_{-0.03}$
IMRPhenomP	$155.28^{+15.99}_{-18.57}$	$1.20^{+0.0}_{-0.0}$	$0.83^{+0.11}_{-0.11}$
IMRPhenomD	$155.21^{+15.98}_{-18.56}$	$1.20^{+0.0}_{-0.0}$	$0.83^{+0.11}_{-0.11}$

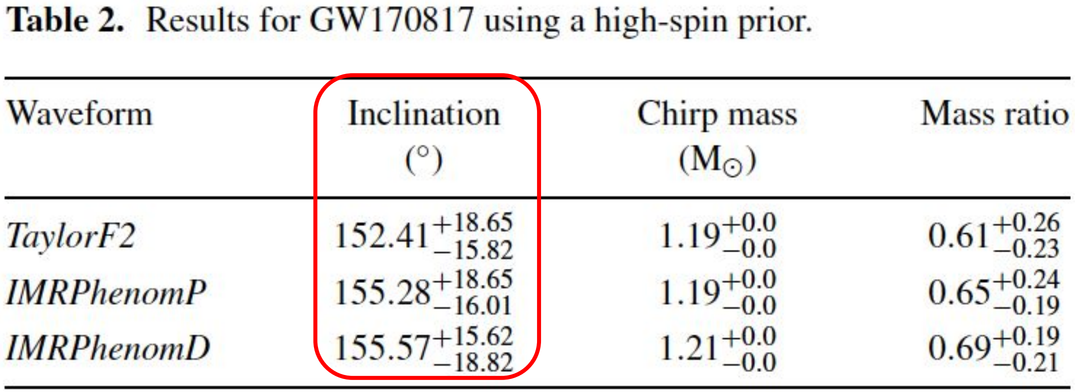

Table 2. Results for GW170817 using a high-spin prior.

Waveform	Inclination (°)	Chirp mass ($M_\odot$)	Mass ratio
TaylorF2	$152.41^{+18.65}_{-15.82}$	$1.19^{+0.0}_{-0.0}$	$0.61^{+0.26}_{-0.23}$
IMRPhenomP	$155.28^{+18.65}_{-16.01}$	$1.19^{+0.0}_{-0.0}$	$0.65^{+0.24}_{-0.19}$
IMRPhenomD	$155.57^{+15.62}_{-18.82}$	$1.21^{+0.0}_{-0.0}$	$0.69^{+0.19}_{-0.21}$

Results on the inclination: GW190425 (BNS)

Table 3. Results for GW190425 using a low-spin prior.

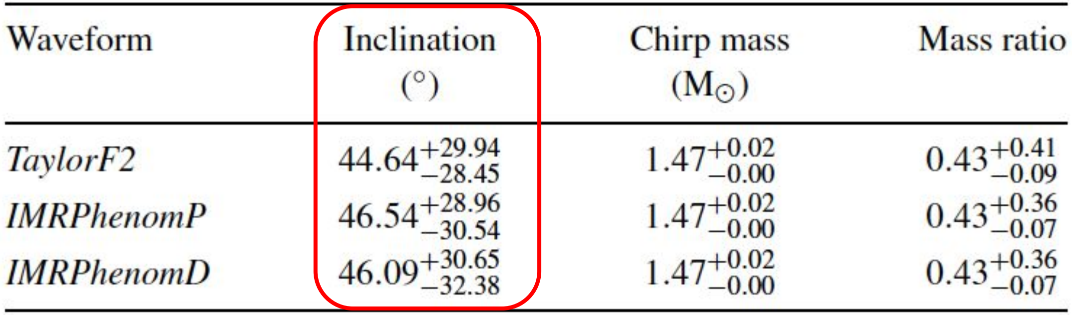

Waveform	Inclination (°)	Chirp mass ($M_\odot$)	Mass ratio
TaylorF2	$44.64^{+29.94}_{-28.45}$	$1.47^{+0.02}_{-0.00}$	$0.43^{+0.41}_{-0.09}$
IMRPhenomP	$46.54^{+28.96}_{-30.54}$	$1.47^{+0.02}_{-0.00}$	$0.43^{+0.36}_{-0.07}$
IMRPhenomD	$46.09^{+30.65}_{-32.38}$	$1.47^{+0.02}_{-0.00}$	$0.43^{+0.36}_{-0.07}$

Table 4. Results for GW190425 using a high-spin prior.

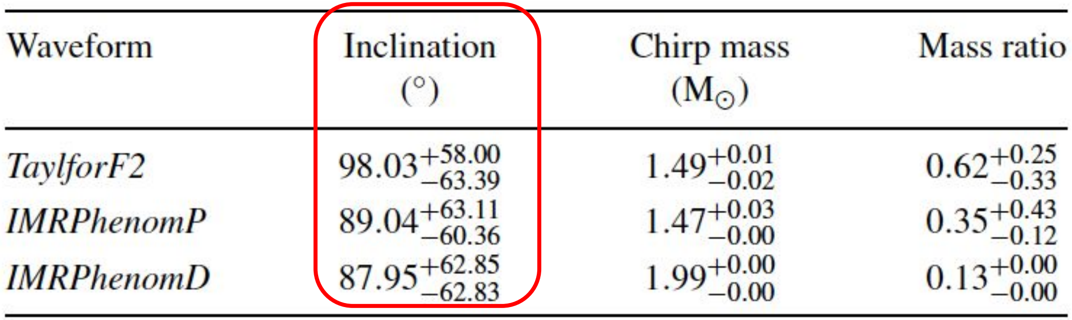

Waveform	Inclination (°)	Chirp mass ($M_\odot$)	Mass ratio
TaylforF2	$98.03^{+58.00}_{-63.39}$	$1.49^{+0.01}_{-0.02}$	$0.62^{+0.25}_{-0.33}$
IMRPhenomP	$89.04^{+63.11}_{-60.36}$	$1.47^{+0.03}_{-0.00}$	$0.35^{+0.43}_{-0.12}$
IMRPhenomD	$87.95^{+62.85}_{-62.83}$	$1.99^{+0.00}_{-0.00}$	$0.13^{+0.00}_{-0.00}$

Results on the inclination: GW190917 (BHNS)

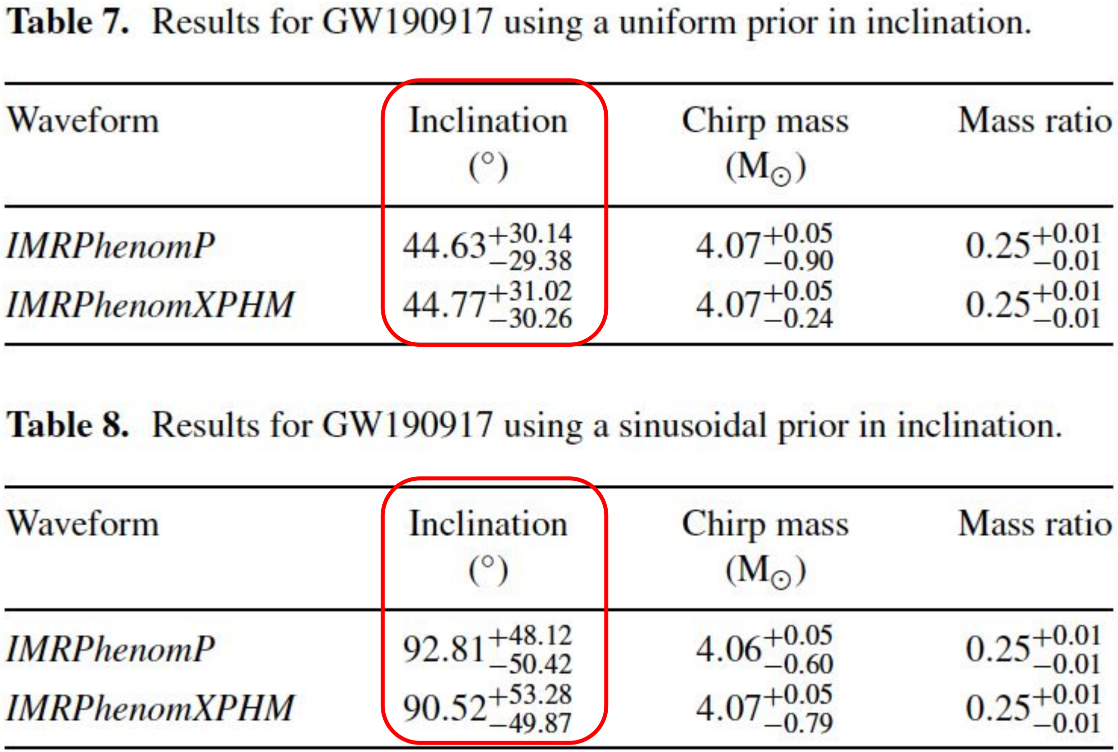

Table 7. Results for GW190917 using a uniform prior in inclination.

Waveform	Inclination (°)	Chirp mass ($M_\odot$)	Mass ratio
IMRPhenomP	$44.63^{+30.14}_{-29.38}$	$4.07^{+0.05}_{-0.90}$	$0.25^{+0.01}_{-0.01}$
IMRPhenomXPHM	$44.77^{+31.02}_{-30.26}$	$4.07^{+0.05}_{-0.24}$	$0.25^{+0.01}_{-0.01}$

Table 8. Results for GW190917 using a sinusoidal prior in inclination.

Waveform	Inclination (°)	Chirp mass ($M_\odot$)	Mass ratio
IMRPhenomP	$92.81^{+48.12}_{-50.42}$	$4.06^{+0.05}_{-0.60}$	$0.25^{+0.01}_{-0.01}$
IMRPhenomXPHM	$90.52^{+53.28}_{-49.87}$	$4.07^{+0.05}_{-0.79}$	$0.25^{+0.01}_{-0.01}$

Inclination angle estimates for BHNS mergers GW200115 and GW190917 with priors uniform in the inclination from $0° \leq \iota \leq 90°$ a prior with sinusoidal distribution from 0° to 360°

Results on the inclination: GW200115 (BHNS)

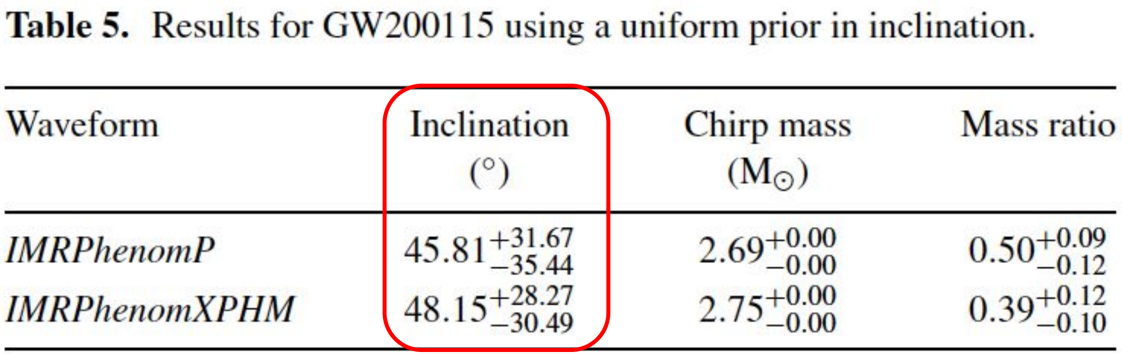

Table 5. Results for GW200115 using a uniform prior in inclination.

Waveform	Inclination (°)	Chirp mass ($M_\odot$)	Mass ratio
IMRPhenomP	$45.81^{+31.67}_{-35.44}$	$2.69^{+0.00}_{-0.00}$	$0.50^{+0.09}_{-0.12}$
IMRPhenomXPHM	$48.15^{+28.27}_{-30.49}$	$2.75^{+0.00}_{-0.00}$	$0.39^{+0.12}_{-0.10}$

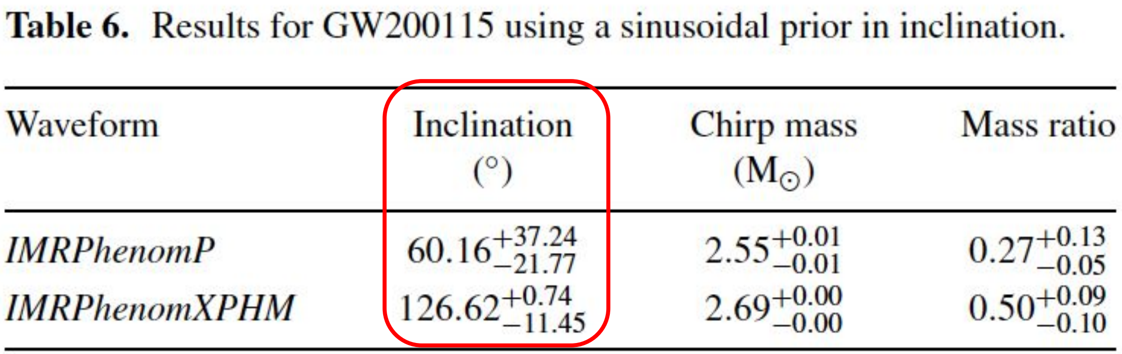

Table 6. Results for GW200115 using a sinusoidal prior in inclination.

Waveform	Inclination (°)	Chirp mass ($M_\odot$)	Mass ratio
IMRPhenomP	$60.16^{+37.24}_{-21.77}$	$2.55^{+0.01}_{-0.01}$	$0.27^{+0.13}_{-0.05}$
IMRPhenomXPHM	$126.62^{+0.74}_{-11.45}$	$2.69^{+0.00}_{-0.00}$	$0.50^{+0.09}_{-0.10}$

Inclination angle estimates for BHNS mergers GW200115 and GW190917 with priors uniform in the inclination from $0° \leq \iota \leq 90°$ a prior with sinusoidal distribution from 0° to 360°

Detection rate of GW events

- The range for a BNS or BHNS system with component masses m_1 and m_2 is found using GWINC
- Using the local rates of BNS and BHNS from Burns (2020)

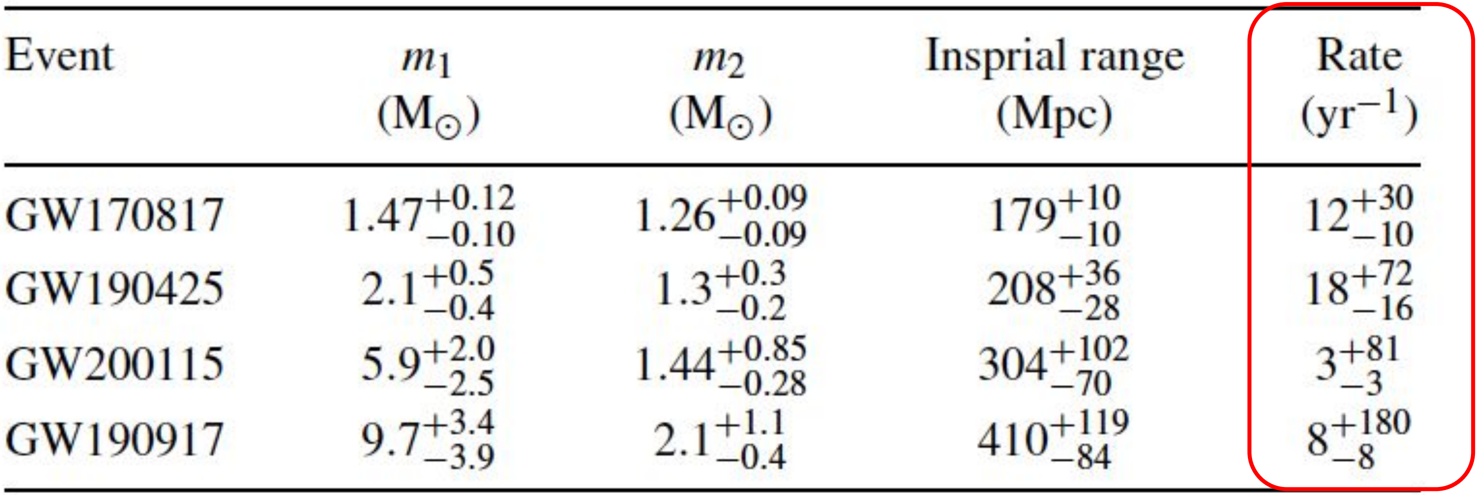

Event	m_1 ($M_\odot$)	m_2 ($M_\odot$)	Insprial range (Mpc)	Rate (yr^{-1})
GW170817	$1.47^{+0.12}_{-0.10}$	$1.26^{+0.09}_{-0.09}$	179^{+10}_{-10}	12^{+30}_{-10}
GW190425	$2.1^{+0.5}_{-0.4}$	$1.3^{+0.3}_{-0.2}$	208^{+36}_{-28}	18^{+72}_{-16}
GW200115	$5.9^{+2.0}_{-2.5}$	$1.44^{+0.85}_{-0.28}$	304^{+102}_{-70}	3^{+81}_{-3}
GW190917	$9.7^{+3.4}_{-3.9}$	$2.1^{+1.1}_{-0.4}$	410^{+119}_{-84}	8^{+180}_{-8}

Joint GW-GRB detection rate

The orbital inclination angle in the 3 GW events was likely such that a short GRB (if formed) was pointing away from our direction.

Joint GW-GRB detection rate

The orbital inclination angle in the 3 GW events was likely such that a short GRB (if formed) was pointing away from our direction.

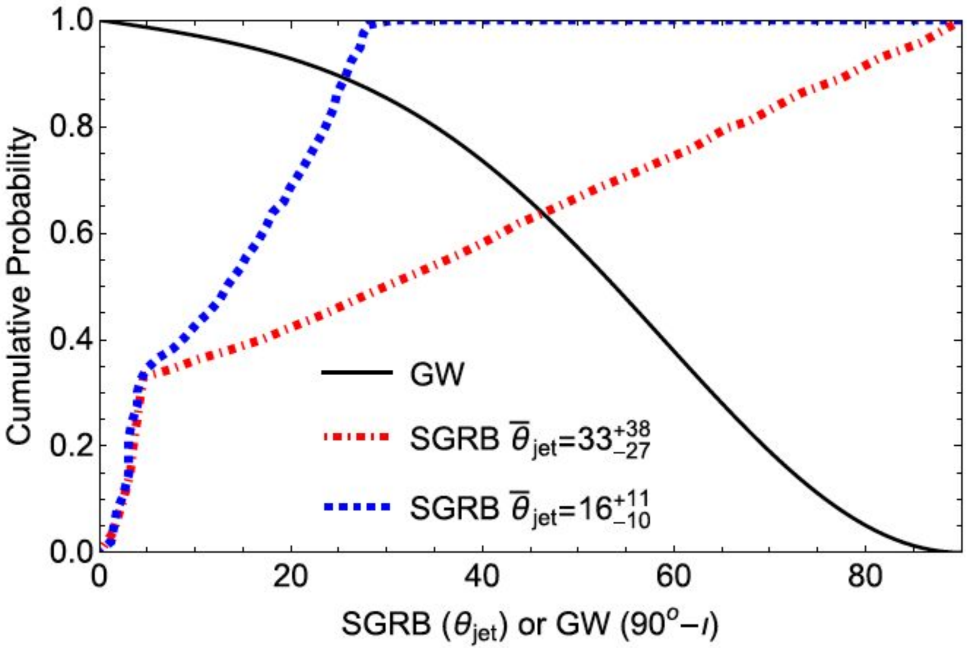

Cumulative probability distributions (CPDs) for SGRB emission and GWs from BNS mergers as a function of SGRB jet opening angle and 90° - ι, where ι is inclination of the binary. The CDPs have been adapted from *Fong+2015* where the maximum jet opening angle was 30° (blue dashed line) and 90° (red dashed curve)

Joint GW-GRB detection rate

The orbital inclination angle in the 3 GW events was likely such that a short GRB (if formed) was pointing away from our direction.

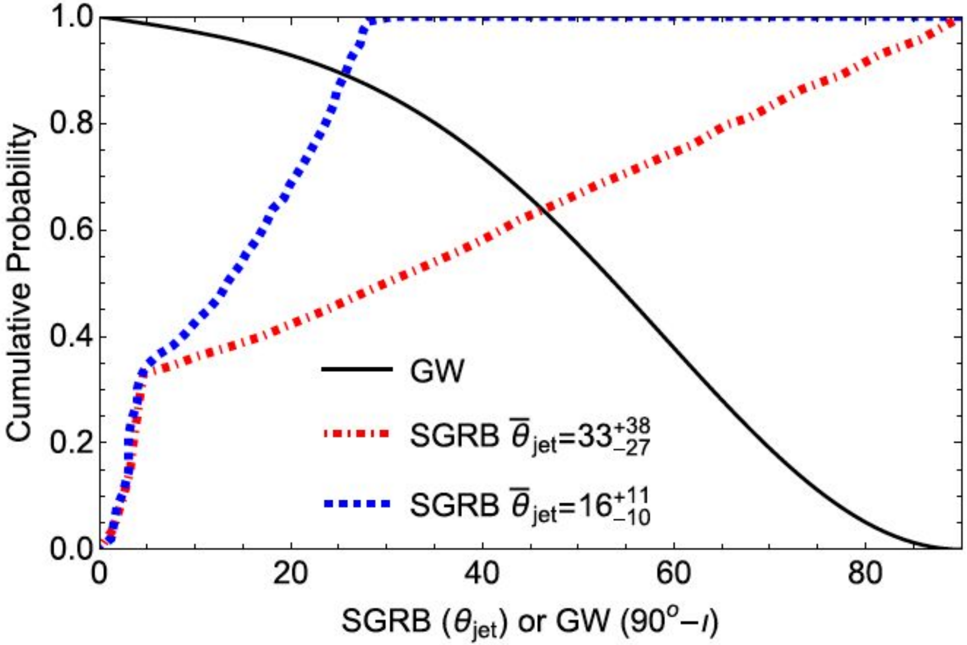

Cumulative probability distributions (CPDs) for SGRB emission and GWs from BNS mergers as a function of SGRB jet opening angle and 90° - ι, where ι is inclination of the binary. The CDPs have been adapted from *Fong+2015* where the maximum jet opening angle was 30° (blue dashed line) and 90° (red dashed curve)

Probability of short GRB detection is ~ 1/2 of every BNS or BHNS event for 33° jet

Conclusions

- The results obtained for the inclination angles of GW events GW190425, GW190917 and GW200115 all suggest inclinations greater than 33°.
- However, there are very large uncertainties on the median values for inclination obtained here. This is due to the luminosity distance inclination angle degeneracy.
- Without an independent means of constraining the luminosity distance, this degeneracy can't be broken.
- Our findings still support current estimates for joint detection rate in O3.

Thank you!